

# Analysis of Acid-Soluble Glycogen in Pork Extracts of Two *PRKAG3* Genotypes by $^1\text{H}$ Liquid-State NMR Spectroscopy and Biochemical Methods

Flemming H. Larsen,<sup>\*,†</sup> Birgitta Essén-Gustavsson,<sup>§</sup> Marianne Jensen-Waern,<sup>§</sup> René Lametsch,<sup>†</sup> Anders H. Karlsson,<sup>†</sup> and Gunilla Lindahl<sup>†,‡</sup>

<sup>†</sup>Department of Food Science, University of Copenhagen, Rolighedsvej 30, DK-1958 Frederiksberg C, Denmark

<sup>‡</sup>Department of Food Science and <sup>§</sup>Department of Clinical Sciences, Swedish University of Agricultural Sciences, P.O. Box 7051, SE-750 07 Uppsala, Sweden

**ABSTRACT:** Meat extracts with acid-soluble glycogen (macroglycogen) from *M. longissimus dorsi* of carriers and noncarriers of the *PRKAG3* mutation ( $RN^-$  and  $m^+$  genotype) were analyzed by both  $^1\text{H}$  liquid-state NMR spectroscopy and a biochemical method. The  $^1\text{H}$  NMR analysis revealed that shorter polymers (dimers, trimers, etc.) of  $\alpha$ -1,4-linked glucose were generated 24–48 h post-mortem. This is not possible to elucidate with the biochemical method, by which only the total amount of hydrolyzed glucose residues is determined. The shorter polymers were primarily formed in carriers of the *PRKAG3* mutation, suggesting different post-mortem glycogen degradation mechanisms in the two genotypes.

**KEYWORDS:** glycogen,  $^1\text{H}$  nuclear magnetic resonance ( $^1\text{H}$  NMR), enzymatic analysis, pork, *RN*-gene, *PRKAG3* mutation

## INTRODUCTION

Glycogen is the cellular energy storage molecule in animals and serves the same purpose as starch does in plants. Both starch and glycogen are  $\alpha$ -linked polymers of glucose, but whereas starch is composed of linear amylose and more branched amylopectin, glycogen is a large branched polymer of glucose units, similar to amylopectin, built up on a core protein, glycogenin.<sup>1</sup>

Glycogen has been divided into two molecular subgroups according to its solubility in trichloroacetic acid or perchloric acid: acid-insoluble glycogen, called proglycogen, with a protein content of about 10% (molecular weight 400 kDa) and acid-soluble glycogen, called macroglycogen (molecular weight  $10^7$  Da) with only 0.35% protein content.<sup>1</sup> Methods for the analysis of glycogen in biological tissues are traditionally based on the hydrolysis of glycogen to glucose units either by acid or enzymatic hydrolysis. Total glycogen as well as pro- and macroglycogen have reliably been measured by both of these methods.<sup>2</sup> However, these biochemical methods do not reveal the actual size and size distribution as well as the configuration or structure of the glycogen molecules. By  $^1\text{H}$  liquid-state nuclear magnetic resonance (NMR) spectroscopy hydrogens in various chemical environments in solution can be identified and quantified, for example, the anomeric proton involved in the  $\alpha$ -1,4 glucosidic bond in glycogen. Previously, this approach has been used for structural analysis of rabbit liver glycogen.<sup>3</sup>

Recent microscopy studies<sup>4,5</sup> demonstrated that two kind of particles can be present in glycogen:  $\beta$ -particles having diameters in the range of 10–30 nm and supramolecular complexes of  $\beta$ -particles, the so-called  $\alpha$ -particles, having diameters up to 300 nm. The  $\alpha$ -particles are so far only observed in liver glycogen, whereas glycogen from skeletal muscles contain only  $\beta$ -particles.<sup>5</sup> Similar to amylopectin, the glucose units in glycogen are connected by linear chain  $\alpha$ -1,4 and branched  $\alpha$ -1,6 glucosidic bonds. The glycogen molecule is formed by two different

kinds of chains, A- and B-chains.<sup>4</sup> The A-chains are not branched, having only  $\alpha$ -1,4 bonds, whereas the B-chains are branched, each of them with two branching points with  $\alpha$ -1,6 bonds, which create new either A- or B-chains. There are four glucose residues between the branches and a tail of approximately four residues after the second branch in the B-chains. The glycogen molecule is spherical and organized into concentric tiers. Every B-chain is in the inner tiers, and every A-chain is within the outer tier. Each A- or B-chain has 12–14 glucose residues, and there are 12 tiers in a molecule. The number of chains in any tier is twice that of the previous one, as a consequence of two branching points at each chain.<sup>6</sup>

The dominant *PRKAG3* mutation (previously known as the *RN^-* mutation) in pigs of the Hampshire breed results in very high glycogen content, especially in glycolytic muscles, compared with the wild type Hampshire pigs.<sup>7</sup> Furthermore, the post-mortem pH decline has been shown to be slightly faster and the ultimate pH lower in *M. longissimus dorsi* (LD) of carriers of the *PRKAG3* mutation compared with noncarriers.<sup>8–11</sup> Essén-Gustavsson et al.<sup>12</sup> studied post-mortem degradation of total glycogen in LD of carriers and noncarriers of the *PRKAG3* mutation using a biochemical method. As expected, they found a higher glycogen content in carriers compared with noncarriers of the *PRKAG3* mutation, but the amount of glycogen degraded from 10 min to 24 h post-mortem did not differ between the genotypes. Samples of LD from the same pigs as in the study of Essén-Gustavsson et al.<sup>12</sup> were in the present study homogenized with perchloric acid and centrifuged, and the soluble glycogen in the supernatant (macroglycogen) was then analyzed

**Received:** May 9, 2011

**Revised:** October 14, 2011

**Accepted:** October 17, 2011

**Published:** October 17, 2011

by both  $^1\text{H}$  liquid-state NMR spectroscopy and a biochemical method.  $^1\text{H}$  NMR provides detailed information about the molecular composition of the sample, whereas the glucose and the glycogen content are determined by the biochemical method. The study aims at comparing the information provided by these two methods concerning glycogen and glycogen degradation in post-mortem muscles from either carriers or noncarriers of the *PRKAG3* mutation.

## MATERIALS AND METHODS

**Animal Material.** Eight clinically healthy pigs (Yorkshire/Swedish Landrace  $\times$  Hampshire), four carriers and four noncarriers of the *PRKAG3* mutation (earlier denoted  $RN^-$  and  $rn^+$  genotypes, respectively) shown by DNA analysis on the blood,<sup>13</sup> were used in the present study. The pigs were housed in pens (four pigs/pen) with straw as bedding. They were fed a commercial finisher diet ad libitum and had free access to water. The pigs were killed with a captive bolt and exsanguinated at a live weight of  $67 \pm 13$  kg. Samples of LD were collected at different times post-mortem, immediately frozen in liquid nitrogen, and stored at  $-80^\circ\text{C}$  until analysis. The first two samples were taken within 24 min post-mortem, and then samples were taken at 30 min and 1, 2, 24, and 48 h post-mortem. For three pigs (two *PRKAG3* carriers and one noncarrier) no samples 24 h post-mortem were collected. At 2 h post-mortem only limited amounts of sample were collected from one of the *PRKAG3* carriers (not identical to the two with missing 24 h samples), which did not permit analysis in duplicate. This sample set was denoted sample set A. Additional samples from 12 pigs, 6 carriers and 6 noncarriers of *PRKAG3* mutation, were collected from a commercial slaughterhouse. The samples were taken 48 h post-mortem, immediately frozen in liquid nitrogen, and stored at  $-80^\circ\text{C}$  until analysis. This sample set was denoted sample set B. The genotype was determined by DNA analysis on muscle samples.<sup>13</sup>

**Preparation of Meat Extracts.** Two grams of finely cut frozen meat was directly without thawing homogenized with 10 mL of cold 0.6 M perchloric acid (Merck KGaA, Darmstadt, Germany) on ice with an Ultra-Turrax T25 (Janke & Kunkel, GmbH, Germany) for 50 s. The homogenate was centrifuged at 5000g and  $4^\circ\text{C}$  for 20 min. The supernatant was used as meat extract in the further analysis.

**Biochemical Analysis.** Glycogen and the sum of glucose and glucose-6-phosphate (G-6-P) were determined in the meat extracts. The analysis was performed as described by Talmant et al.<sup>14</sup> and Keppler and Decker.<sup>15</sup> Glycogen was hydrolyzed to glucose units with amyloglycosidase (Sigma-Aldrich) at pH 5 and  $37^\circ\text{C}$  for 2 h. Then 3 M perchloric acid was added to inactivate the enzyme, and the sample was centrifuged at 2000g for 10 min. The supernatant was used for the simultaneous determination of glucose and G-6-P using a commercial kit Glucose Hexokinase FS (DiaSys Diagnostic Systems GmbH, Germany) and glucose standard solution (Sigma-Aldrich). In addition, the sum of free glucose and G-6-P was determined in the supernatant without the hydrolysis step. Glycogen was determined as the difference in glucose content between hydrolyzed and nonhydrolyzed samples. The results were expressed as micromoles of glucose per gram of wet muscle.

**pH Measurements.** The pH of the meat was determined using the method of Bendall<sup>16</sup> in a slightly modified version. One gram of meat was homogenized in 6 mL of cold homogenization solution (0.05 M KCl, 5 mM iodoacetamide), and the pH was measured using a Knick Portamess 751 Calimatic pH-meter (Knick Elektronische Mess Geräte GmbH & Co., Berlin, Germany) immediately after the homogenization.

**Detection of Glucose Polymers.** Meat extracts obtained from sample set B were filtered using centrifuge filters with 30 kDa molecular weight cutoff (Amicon Centriplus YM-30, Millipore). The filtrates were collected and analyzed by  $^1\text{H}$  NMR spectroscopy.

**Glycogen Hydrolysis.** Thirty microliters of amyloglycosidase (0.05 mg/mL, 0.2 M  $\text{CH}_3\text{COONa}$ ) (Sigma-Aldrich) was mixed with  $495\ \mu\text{L}$  of meat extract and  $55\ \mu\text{L}$  of  $\text{D}_2\text{O}$  containing 5.8 mM TSP- $d_4$ . The glycogen hydrolysis was followed over time at 298 K using  $^1\text{H}$  NMR spectroscopy.

**NMR Spectroscopy.** Samples for  $^1\text{H}$  NMR spectroscopy were prepared in 5 mm (od) NMR sample tubes by mixing  $495\ \mu\text{L}$  of meat extract (see above) with  $55\ \mu\text{L}$  of  $\text{D}_2\text{O}$  containing 5.8 mM of TSP- $d_4$ . All samples were analyzed using a Bruker Avance 400 spectrometer operating at a Larmor frequency of 400.13 MHz for  $^1\text{H}$  using a double-tuned inverse detection BBI probe equipped with Z-gradients. All samples were analyzed at a temperature of 298 K. One-dimensional (1D)  $^1\text{H}$  experiments were performed using the *zgpgpr* pulse sequence (presaturation followed by a composite  $90^\circ$  pulse)<sup>17</sup> to achieve sufficient water suppression. For each sample 64 scans were acquired using a recycle delay of 5 s, a spectral width of 8278.15 Hz, and an acquisition time of 1.98 s. Prior to Fourier transformation, the FIDs were apodized by Lorentzian line broadening of 0.3 Hz and zero-filled to 64K data points. All spectra were subsequently referenced to TSP- $d_4$  at 0.0 ppm. Before data analysis the residual water resonance (4.72–5.12 ppm) was removed from the spectra, and the remaining part of the spectrum was carefully baseline corrected. All spectra of samples from sample set A were recorded on two different extracts of each sample (except one at 2 h post-mortem), whereas the spectra of sample set B were recorded on one sample for each animal.

To support assignments of various resonances, a homonuclear  $^1\text{H}$ – $^1\text{H}$  COSY spectrum using the *cosygpmpfj*<sup>18</sup> pulse sequence and a heteronuclear  $^1\text{H}$ – $^{13}\text{C}$  HSQC (*hsqcphpr*) spectrum of one sample from sample set A were acquired.

**Data Analysis.** The 1D  $^1\text{H}$  NMR data were subjected to principal component analysis (PCA) using the *plstoolbox* 5.5.1 in Matlab 7.9.0.529. Prior to PCA, the spectra were aligned<sup>19</sup> and mean centered, and the PCA was performed with full cross-validation. Regression analysis was performed by the built-in routines in Gnuplot 4.0 ([www.gnuplot.info](http://www.gnuplot.info)).

Analysis of variance was carried out with Statistical Analysis System version 9.1 (SAS Institute Inc., Cary, NC). The MIXED procedure was applied for the calculation of least-squares means (LSM) and standard errors (SE), and the option PDIF was used for the calculation of significant differences between LSM. Degrees of freedom were estimated with the Satterthwaite method. The initial statistical model included genotype and time point post-mortem and their interaction as fixed effects and animal within genotype as random effect. The interaction between the fixed effects genotype and time post-mortem was not significant for any of the parameters. The effect of time post-mortem was therefore analyzed within each genotype (carriers and noncarriers of the *PRKAG3* mutation) separately using a model with time post-mortem as fixed effect and animal as random effect. Differences between the genotypes were analyzed separately at each time point post-mortem (<0.4, 0.5, 1, 2, 24, and 48 h) using a model with genotype as fixed effect and animal as random effect.

## RESULTS

Examples of  $^1\text{H}$  NMR spectra of extracted meat samples from a carrier of the *PRKAG3* mutation collected 17 min (lower spectra) and 48 h post-mortem (upper spectra) are displayed in Figure 1. Resonances from lactic acid, creatine, and carnosine can be easily identified in Figure 1A using the assignments in Table 1. Besides differences induced by pH effects, the chemical shifts are in accordance with Arus et al.<sup>20</sup> In Figure 1B a zoom on the spectral range 6.1–9.4 ppm is displayed. Two intense resonances from the histidine ring in carnosine and a number of less intense resonances were observed. The intensity of these resonances is

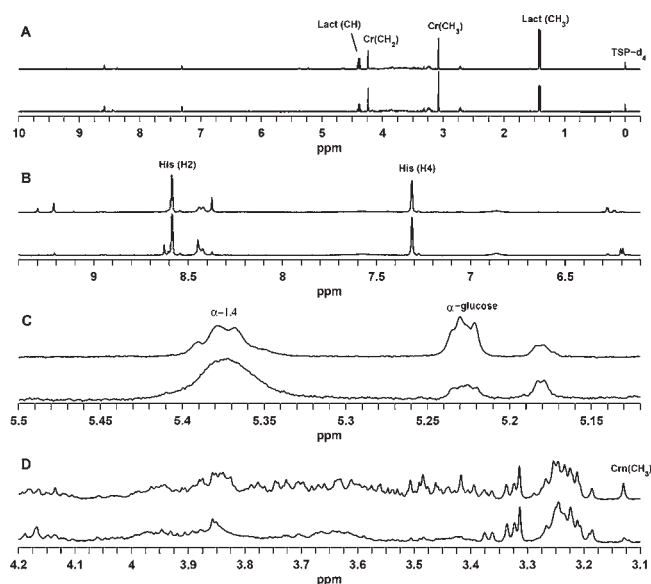


**Figure 1.**  $^1\text{H}$  NMR spectra of extracts from *M. longissimus dorsi* in a *PRKAG3* mutation carrier ( $RN^-$ ) from sample set A displaying different spectral regions: (A)  $-0.25$  to  $10.0$  ppm; (B)  $6.1$ – $9.4$  ppm; (C)  $5.12$ – $5.5$  ppm; (D)  $3.1$ – $4.2$  ppm. For each region the upper spectra originate from 48 h post mortem and the lower spectra from 17 min post mortem. Annotation is in accordance with assignments in Table 1. Lact, lactate; Cr, creatine; Crn, creatinine; His, histidine.

**Table 1.** Assignment of  $^1\text{H}$  Chemical Shifts of Perchloric Acid Extracts

compound	$^1\text{H}$ chemical shifts <sup>a</sup> (ppm)
$\alpha$ -1,4-linked glucose polymers (e.g., glycogen)	5.37, 3.62, 3.97, 3.64, 3.85, 3.84
$\alpha$ -glucose	5.23 (d)
creatine (Cr)	4.24 (s), 3.07 (s)
creatinine (Crn)	4.29 (s), 3.13 (s)
lactate (Lact)	4.39 (q), 1.41 (d)
histidine (His) from, e.g., carnosine	8.59 (s), 7.31 (s)

<sup>a</sup>Chemical shifts are reported relative to  $\text{TSP-}d_4$ . Multiplicity of resonances: s, singlet; d, doublet; t, triplet; q, quartet; m, multiplet. Resonances from glycogen and other  $\alpha$ -1,4-linked polymers were either too broad or overlapped by other resonances, which prevented determination of coupling patterns due to  $J$ -couplings.

significantly different in the upper and lower spectra, reflecting changes as a function of time. Figure 1C focuses on the region  $5.12$ – $5.5$  ppm in which the resonances originating from anomeric protons in  $\alpha$ -glucose and  $\alpha$ -1,4-linked glucose units, as in glycogen, are present. The chemical shift of the anomeric proton is significantly different from other protons in the glucose unit because the anomeric proton is the only one bonded to a carbon attached to two oxygens. In glucose polymers (dimers, trimers, etc.) the exact chemical shift of the anomeric protons depends on the conformation of the glucosidic bonds and allows for distinction of, for example, maltose,<sup>21</sup> maltotriose,<sup>22</sup> and starch.<sup>23</sup> Significant differences in the intensities and line shapes between the two spectra for  $\alpha$ -glucose and  $\alpha$ -1,4-linked glucose units are observed, indicating large differences in the carbohydrate

composition of the extracts at the two time points. In Figure 1D the region  $3.1$ – $4.2$  ppm is displayed. A number of differences between the two spectra in the region  $3.4$ – $4.0$  ppm reflected the difference in carbohydrate composition, whereas differences in creatinine level were observed between  $3.1$  and  $3.15$  ppm.

Several components were identified and quantified in the  $^1\text{H}$  NMR spectra, and some of the results are displayed in the two left columns of Figure 2. As can be seen lactate (Figure 2C,F),  $\alpha$ -glucose (Figure 2B,E), and  $\alpha$ -1,4-linked glucose units (Figure 2A,D) were quantified. The content of  $\alpha$ -1,4-linked glucose units was significantly higher ( $P < 0.05$ ) in carriers of the *PRKAG3* mutation compared to the noncarriers at all time points post-mortem. Because the  $\alpha$ -1,4-linked glucose units are mainly found in glycogen, this is in accordance with our expectations. The glucose levels (Figure 2B,E) increased slowly during the first 2 h, whereas a strong increase was observed between 2 and 24 h. This increase was more prominent for carriers of the *PRKAG3* mutation than for noncarriers. The lactate level (Figure 2C,F) increased slowly during the first 2 h in noncarriers. In carriers of the *PRKAG3* mutation the lactate level remained constant up to 1 h post-mortem followed by an increase between 1 and 2 h post-mortem. However, no significant differences in lactate levels between the genotypes were found at any time point post-mortem. After 24 h, the lactate level was about twice the initial level in both genotypes, and this level was maintained after 48 h. The decrease in pH value (Table 2) exhibited a similar behavior as the lactate content with a marked decrease between 0.5 and 2 h in carriers of the *PRKAG3* mutation, but a smoother decrease in noncarriers. No significant differences in pH between the genotypes were found at any time point post-mortem. For comparison, the two right columns of Figure 2 display glycogen (Figure 2G,I) and glucose levels (Figure 2H,J) obtained from the biochemical methods. Similar to the  $^1\text{H}$  NMR results (Figure 2B,E), increased glucose levels as a function of time post-mortem was observed by the biochemical method. The glycogen levels obtained by the biochemical method (Figure 2G,I) showed a significant reduction at more than 2 h post-mortem in both genotypes. In principle, the reduction in glycogen level determined by the biochemical method should be strongly correlated to the content of  $\alpha$ -1,4-linked glucose units observed by  $^1\text{H}$  NMR, but beyond 24 h post-mortem discrepancies between results by the two methods were observed. According to  $^1\text{H}$  NMR results the level of  $\alpha$ -1,4-linked glucose units increased from 24 to 48 h post-mortem, whereas the glycogen level determined by the biochemical method either slightly decreased or remained stable between 24 and 48 h (Figure 2A,D). In this context it must be noted that resonances from anomeric protons in  $\alpha$ -1,4-linked glucose units such as dimers, trimers, etc., would also contribute to the spectral region of the  $\alpha$ -1,4 protons. This indicates that a range of molecules with different sizes were present. Further support of this observation was obtained from Figure 3, in which PCA score plots and corresponding loadings are displayed for the spectral region  $5.20$ – $5.45$  ppm. The samples are clearly grouped in carriers and noncarriers of the *PRKAG3* mutation in the score plots. This distinction is clearest for the samples collected up to 2 h post-mortem (Figure 3A), but a similar tendency is observed when the samples from 24 and 48 h are included (Figure 3C). From an inspection of the corresponding loadings (Figure 3B), it is noted that principal component (PC) 1 in the  $<0.4$ – $2$  h plot is mainly due to  $\alpha$ -1,4-linked glucose unit from glycogen (broad peak

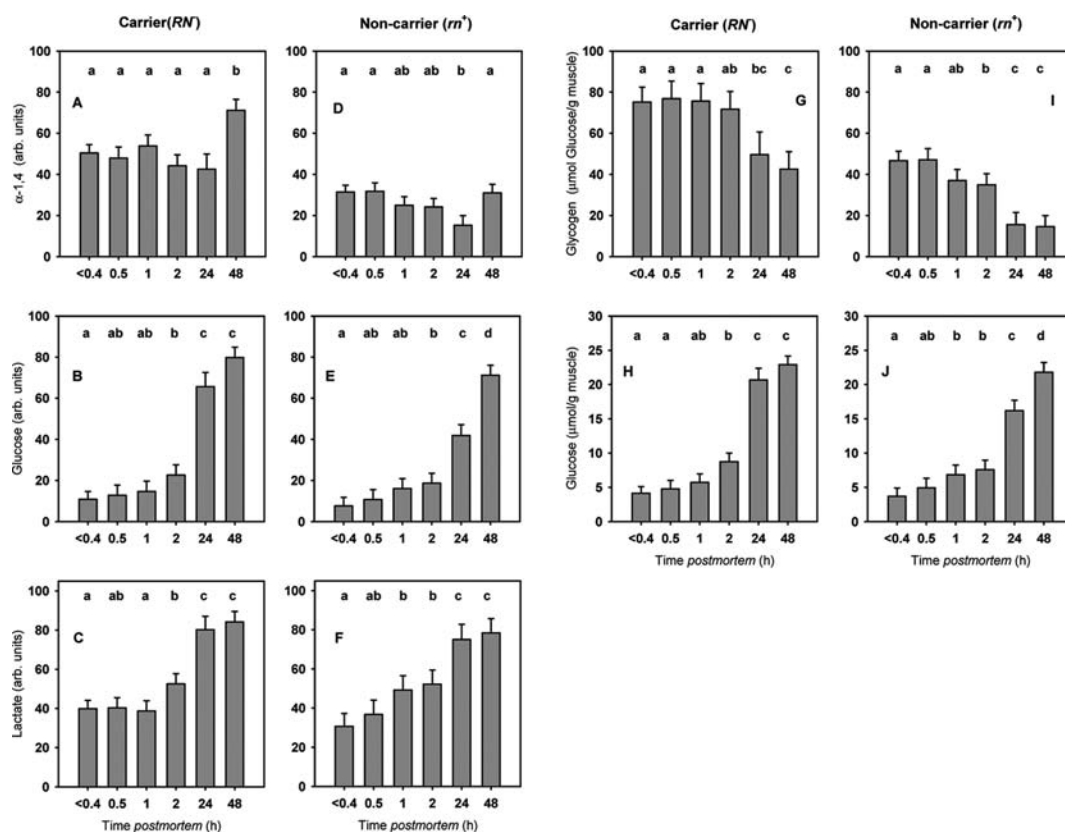


**Figure 2.** Integrated signal intensities (arbitrary units) from the  $^1\text{H}$  NMR spectra of sample set A (two left columns) for lactate (C, F), glucose (B, E), and  $\alpha$ -1,4 (A, D) and biochemical determination (two right columns) of the glucose (H, J) and glycogen (G, I) contents. All contents were determined as a function of time post-mortem for carriers ( $RN^-$ ) and noncarriers ( $rn^+$ ) of the *PRKAG3* mutation, respectively. Least-squares means and standard errors. Different letters (a–d) within the same trait and genotype indicate significant differences,  $P < 0.05$ .

**Table 2.** pH Values at Different Time Points Post-mortem in *M. longissimus dorsi* of Carriers ( $RN^-$ ) and Noncarriers ( $rn^+$ ) of the *PRKAG3* Mutation<sup>a</sup>

time post-mortem (h)	<i>PRKAG3</i> mutation	
	carrier	noncarrier
<0.4	6.14 ab	6.13 ab
0.5	6.23 a	6.18 a
1	6.22 ab	6.03 bc
2	6.00 b	5.90 c
48	5.59 c	5.62 d
SE	0.09	0.08

<sup>a</sup> Least-squares mean (LSM) and standard error (SE). Significant differences between LSM with different letters within the same column,  $P < 0.05$ .

around 5.37 ppm) and that PC2 is mainly due to  $\alpha$ -glucose (doublet at 5.23 ppm). When the samples from 24 and 48 h post-mortem are included, Figure 3D shows that PC1 represents a mixture of  $\alpha$ -glucose and a peak around 5.37 that exhibits multiplet structure or a pattern from overlapping doublets. PC2 represents a linear combination of  $\alpha$ -glucose and glycogen (broad peak). The multiplet structure of the resonance at 5.37 ppm in PC1 indicates the presence of a short-chain  $\alpha$ -1,4-linked glucose unit as is found in maltose, maltotriose, or even longer chains. These molecules are significantly smaller than glycogen,

and therefore they tumble more rapidly, and it is possible to observe the anticipated doublet associated with the anomeric protons of the  $\alpha$ -1,4-linked glucose units.

To confirm the generation of shorter glucose polymers, meat extracts obtained from meat collected at 48 h post-mortem were filtered using a filter with a 30 kDa cutoff. Analysis of the filtrates by  $^1\text{H}$  NMR (see Figure 4) confirmed generation of shorter  $\alpha$ -1,4-linked glucose polymers. Comparison of the spectra labeled A and B in Figure 4 suggests that the shorter polymers were primarily formed in carriers of the *PRKAG3* mutation. Only a very small amount of shorter polymers was detected in the spectra from noncarriers that almost only contained glucose. This suggests different post-mortem glycogen degradation mechanisms for carriers and noncarriers.

The correlation of glycogen content determined by the biochemical methods and integrals of the resonance of the  $\alpha$ -1,4-linked glucose units in the  $^1\text{H}$  NMR spectra up to 2 h post-mortem is displayed in Figure 5. A correlation coefficient of 0.93 illustrates a strong relationship between results obtained by the two methods during the first 2 h post-mortem. At later post-mortem periods the results from  $^1\text{H}$  NMR and the biochemical method do not agree. To further explore the reason for this discrepancy, a meat extract mixed with  $\alpha$ -amylase was followed over time by  $^1\text{H}$  NMR spectroscopy. In Figure 6 examples of  $^1\text{H}$  NMR spectra at three different time points after addition of the enzyme is presented. An immediate observation was that the intensity (and integral) of the resonance from  $\alpha$ -glucose (doublet around 5.23 ppm) increased as

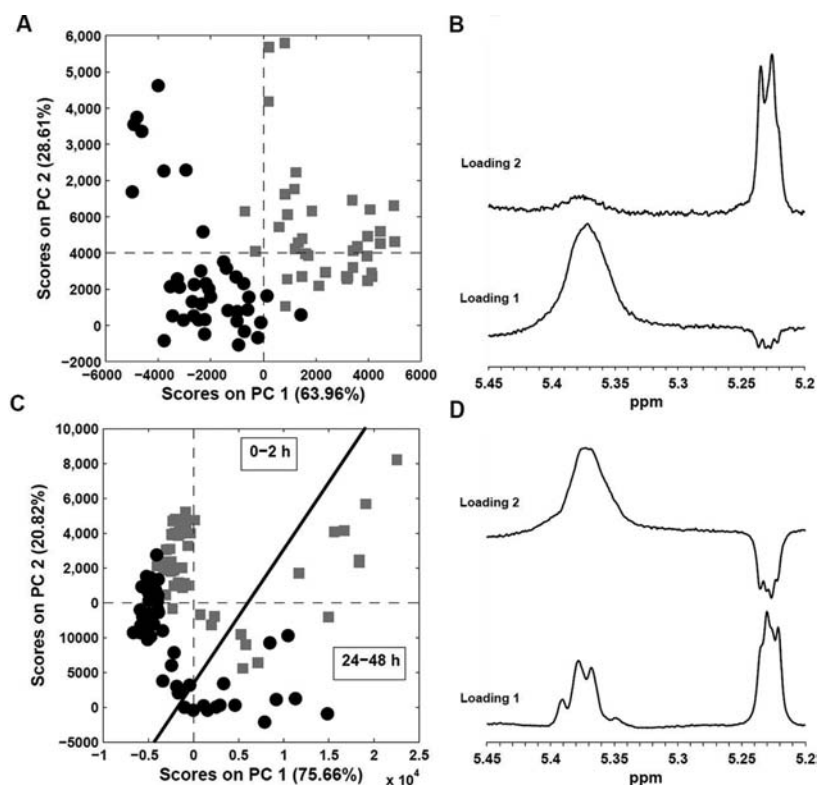


**Figure 3.** Score plots (A, C) and corresponding loadings for components (PC) 1 and PC 2 (B, D) from principal component analysis of the  $^1\text{H}$  NMR spectral region 5.20–5.45 ppm of sample set A including samples either obtained 0–2 h post-mortem (A, B) or all samples (C, D). Samples corresponding to noncarriers of the *PRKAG3* mutation ( $m^+$ ) are marked with a solid black circle, and carriers of the *PRKAG3* mutation ( $RN^-$ ) are marked with gray squares. In panel C a black line separates the samples obtained 0–2 h post-mortem (above the line) and the samples obtained 2–48 h post-mortem (below the line).

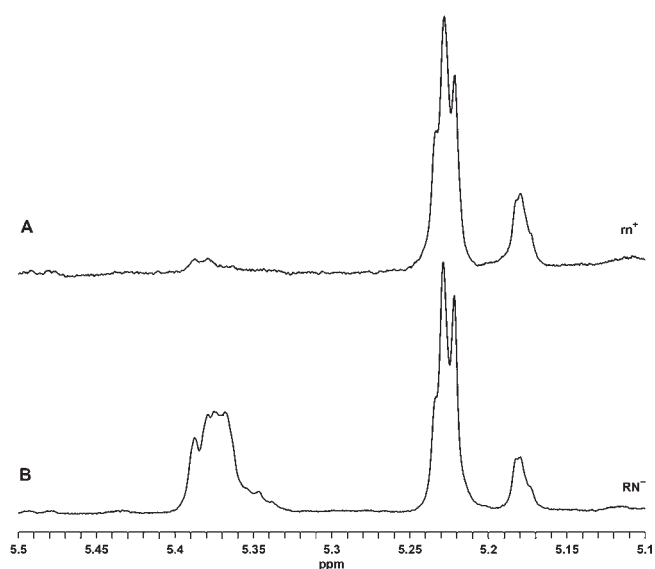


**Figure 4.**  $^1\text{H}$  NMR spectra (average of samples from six pigs each) of meat extracts (sample set B) after filtering through a 30 kDa cutoff filter: (A) extract from noncarriers of the *PRKAG3* mutation ( $m^+$ ); (B) carriers of the *PRKAG3* mutation ( $RN^-$ ).

a function of time, whereas the broad resonance around 5.4 ppm - (glycogen) was reduced. This tendency was expected because  $\alpha$ -amylase breaks down glycogen into glucose, but the increase in

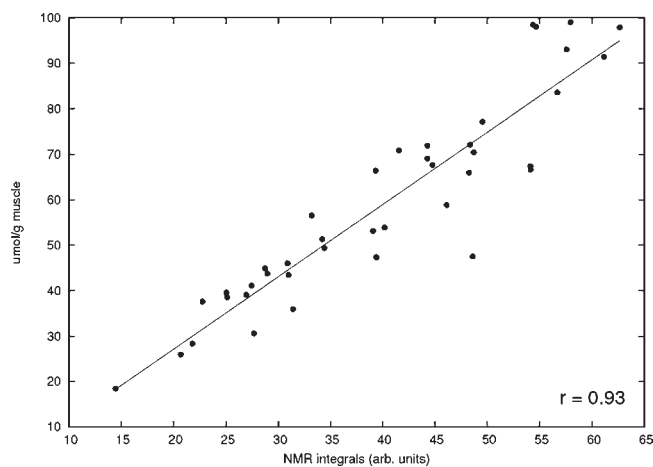


**Figure 5.** Correlation between glycogen content (0–2 h) determined by either biochemical method or  $^1\text{H}$  NMR integrals (5.30–5.45 ppm) of sample set A. All points are an average of two independent measurements.

intensity of the  $\alpha$ -glucose resonance cannot be explained by a corresponding decrease in the resonance of glycogen. The integral of the  $\alpha$ -glucose resonance at 1233 min after addition of enzyme is far beyond the integral of the glycogen and the  $\alpha$ -glucose resonances 7 min after the addition of enzyme, and because the  $\alpha$ -glucose/ $\beta$ -glucose-ratio is 36:64,<sup>24</sup> it is only 36% of the free glucose in the sample that is observed this way. As the only glucose source is

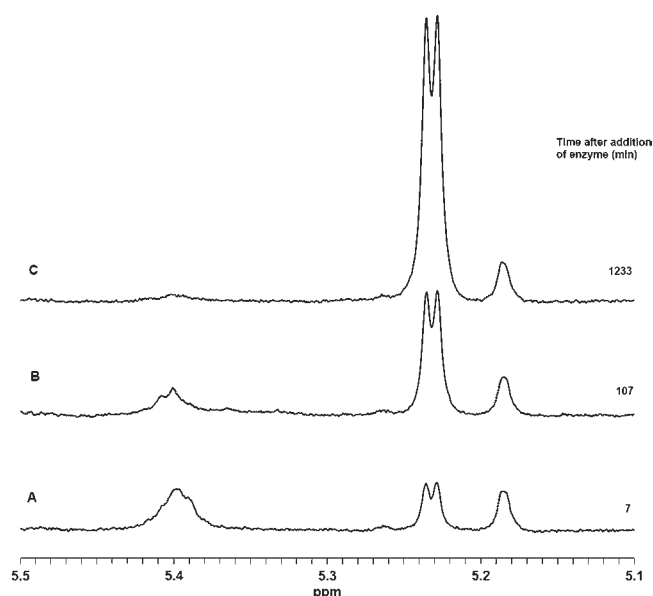


**Figure 6.** Examples of  $^1\text{H}$  NMR spectra from a time series of a meat extract sample (sample from sample set B) mixed with  $\alpha$ -amylase at time = 0 min. The spectra were recorded at 7 min (A), 107 min (B), and 1233 min (C) after addition of the enzyme.

glycogen, this means that not all of the hydrogens in glycogen are observable. If a  $^1\text{H}$  site is to be observable by liquid-state NMR, it must be present in the liquid state. For very large molecules such as pro- and macroglycogen, it is sometimes not possible to describe these as dissolved because some regions of the molecule may be inaccessible for the solvent (presently water). Previously, it has been reported that it was not possible to observe all protons in starch prior to gelatinization due to lack of hydration, whereas all protons were observed in gelatinized starch.<sup>23</sup> Taking the resemblance of glycogen and amylopectin into account, it is highly likely that a similar lack of hydration may occur in some regions of glycogen and thereby prevent observation of glucose residues in these regions by  $^1\text{H}$  NMR. Moreover, slow tumbling of large molecules induce fast relaxation and thereby significant line broadening that hampers detection, as is also observed for proteins.<sup>25</sup>

## DISCUSSION

By  $^1\text{H}$  NMR and the biochemical method it was demonstrated that muscle glycogen stores decrease until 24 h post-mortem. However, the  $^1\text{H}$  NMR results showed an increase in anomeric  $\alpha$ -1,4 protons between 24 and 48 h in the acid-soluble fraction from both genotypes, whereas a constant level or further reduction of glycogen was observed by the biochemical method. This discrepancy cannot be explained by the generation of shorter glucose polymers from macroglycogen as these glucose polymers will also be hydrolyzed during the glycogen assay and contribute to the amount of glycogen. A plausible explanation involves two competing mechanisms: hydration and enzymatic degradation. Hydration is a prerequisite for observation by  $^1\text{H}$  NMR, and, furthermore, water is required for enzymatic activity. The strong correlation between the glycogen content determined by the biochemical method and  $^1\text{H}$  NMR during the first 2 h post-mortem indicates that the fraction of observable  $\alpha$ -1,4-linked glucose polymers is constant during the first 2 h and then increases. At 24 h post-mortem and beyond, a larger fraction of

shorter  $\alpha$ -1,4-linked glucose polymers was observed. It is assumed that this is caused by a change in activity of the enzymes degrading these molecules and thereby a different glycogen degradation mechanism.

The distinction in molecular sizes of  $\alpha$ -1,4-linked glucose polymers was not possible to detect using the biochemical method, because this method determines only the total content of hydrolyzed glucose residues. Compared to the present  $^1\text{H}$  NMR-based method, a conventional sugar analysis would have provided a similar and probably more detailed result, but such an approach would also involve a more extensive sample preparation.

A plausible explanation of the generation of the shorter glucose polymers is that the reduction in pH during post-mortem glycolysis may weaken the walls of lysosomes and facilitate release of lysosomal enzymes.<sup>26</sup> An example of such an enzyme is acid  $\alpha$ -glucosidase (EC 3.2.1.20), which is active at low pH and hydrolyzes  $\alpha$ -1,4 and  $\alpha$ -1,6 linkages in glycogen.<sup>27</sup> Another important enzyme in this context is glycogen debranching enzyme (GDE), which hydrolyzes  $\alpha$ -1,6 linkages in glycogen. GDE is highly affected by temperature but not particularly affected by pH in the range of 5.5–7.0 as found in post-mortem muscle.<sup>28</sup> The activity decreases at lower temperatures and is almost zero below 15 °C. This implicates that the degradation of glycogen is not complete when the temperature is too low for the activity of GDE. The chilling rate of the carcass after slaughter determines when this temperature is achieved. The temperature had decreased to below 15 °C already 3 h post-mortem in a study of Hampshire crossbred pigs slaughtered at a commercial slaughterhouse.<sup>9</sup> Decreased activity of GDE due to low temperature might explain the presence of short  $\alpha$ -1,4-linked glucose chains at 24–48 h post-mortem. It is not known if both hydrolysis and transferase activity of the bifunctional enzyme GDE are reduced at low temperature. Inactivated transferase activity, but active hydrolysis, would result in the release of maltotriose groups, which are too short to be hydrolyzed by phosphorylase. The reduced activity of GDE may also expose a series of shorter  $\alpha$ -1,4-linked glucose polymers to water due to incomplete degradation of branch points in the B-chains of glycogen. Both scenarios would enable observation of either maltotriose or maltotetraose (there are only four glucose units between branch points in the B-chains) by  $^1\text{H}$  NMR as reported in the present study.

Ylä-Ajos et al.<sup>28</sup> studied the activity of GDE from 0.5 to 48 h post-mortem in LD of carriers and noncarriers of the *PRKAG3* mutation of Hampshire crossbred pigs. They found a slow decrease in GDE activity as a function of time post-mortem, but even after 48 h, the activity was still pronounced. However, these activity measurements were performed on meat extracts at 39 °C and are thus not comparable with the low-temperature conditions prevailing in the muscle in the present study. The activity of GDE in that study was significantly lower in noncarriers than in carriers of the *PRKAG3* mutation after 24 and 48 h. Combined with results from the present study, this suggests that the hydrolytic activity in GDE remains for a longer period in carriers of the *PRKAG3* mutation than in noncarriers. In the present work both analytical methods showed a marked increase in the glucose content from 2 to 24 and 48 h post-mortem in both genotypes with no significant differences between the genotypes. This is in agreement with the increase in glucose content of whole muscle extracts (including both pro- and macroglycogen) from 2 to 24 h in LD samples from

the same pigs as in our study.<sup>12</sup> Copenhafer et al.<sup>29</sup> also reported an increased glucose content in whole muscle extracts from 2 to 24 h in both *PRKAG3* genotypes, although at a lower magnitude than in our study. They also reported that a greater amount of total glycogen was hydrolyzed from 0 min to 24 h in carriers compared with noncarriers of the *PRKAG3* mutation. This disagrees with our study and the study of Essén-Gustavsson et al.,<sup>12</sup> in which approximately the same amount of biochemically analyzed glycogen was hydrolyzed in both genotypes.

In conclusion, glycogen contents determined by <sup>1</sup>H NMR and the biochemical method correlated very well on samples up to 2 h post-mortem. Additional information from the <sup>1</sup>H NMR analysis revealed that smaller polymers of  $\alpha$ -1,4-linked glucose units (dimers, trimers, etc.) were generated after 24–48 h post-mortem. This has not been possible to elucidate earlier with the generally used biochemical method, which only analyzes hydrolyzed glucose residues, not anomeric hydrogens in  $\alpha$ -1,4 linked glucose units as with the <sup>1</sup>H NMR method. The shorter polymers were primarily formed in carriers of the *PRKAG3* mutation, with only very small amounts in noncarriers, suggesting different post-mortem glycogen degradation mechanisms.

## AUTHOR INFORMATION

### Corresponding Author

\*Phone: +45 3533 3501. Fax: +45 3533 3245. E-mail: fhl@life.ku.dk.

### Funding Sources

The project was supported by funding from the Danish Research Agency in the Fibimmun project (Project 2105-05-0066) and from the Swedish Research Council for Environment, Agricultural Sciences and Spatial Planning.

## ACKNOWLEDGMENT

We acknowledge Anja Hullberg and Christina Nilsson for sampling of the meat after slaughter, Magdalena M. Żbikowska for performing all of the glycogen analyses, and Linda de Sparra Terkelsen for preparation of samples for glycogen hydrolysis.

## ABBREVIATIONS USED

D<sub>2</sub>O, deuterium oxide; GDE, glycogen debranching enzyme; G-6-P, glucose-6-phosphate; <sup>1</sup>H NMR, <sup>1</sup>H nuclear magnetic resonance spectroscopy; COSY, correlation spectroscopy; HSQC, heteronuclear single-quantum coherence; LD, *M. longissimus dorsi*; PCA, principal component analysis; PC, principal component; *PRKAG3*, a pig gene.

## REFERENCES

- (1) Lomako, J.; Lomako, W. M.; Whelan, W. J. Glycogenin: the primer for mammalian and yeast glycogen synthesis. *Biochim. Biophys. Acta* **2004**, *1673*, 45–55.
- (2) Adamo, K. B.; Graham, T. E. Comparison of traditional measurements with macroglycogen and proglycogen analysis of muscle glycogen. *J. Appl. Physiol.* **1998**, *84*, 908–913.
- (3) Zang, L.-H.; Howseman, A. M.; Shulman, R. G. Assignment of the <sup>1</sup>H chemical shifts of glycogen. *Carbohydr. Res.* **1991**, *220*, 1–9.
- (4) Sullivan, M. A.; Vilaplana, F.; Cave, R. A.; Stapleton, D.; Gray-Weale, A. A.; Gilbert, R. G. Nature of  $\alpha$  and  $\beta$  particles in glycogen using molecular size distributions. *Biomacromolecules* **2010**, *11*, 1094–1100.
- (5) Ryu, J.-H.; Drain, J.; Kim, J. H.; McGee, S.; Gray-Weale, A.; Waddington, L.; Parker, G. J.; Hargreaves, M.; Hoo, S.-H.; Stapleton, D.

Comparative structural analysis of purified glycogen particles from rat liver, human skeletal muscle and commercial preparations. *Int. J. Biol. Macromol.* **2009**, *45*, 478–482.

(6) Meléndez-Hevia, E.; Waddell, T. G.; Shelton, E. D. Optimization of molecular design in the evolution of metabolism: the glycogen molecule. *Biochem. J.* **1993**, *295*, 477–483.

(7) Lundström, K.; Andersson, L. The effect of the *RN*<sup>-</sup> allele on meat quality and how the gene was discovered. In *Proceedings 54th Annual Reciprocal Meat Conference*; American Meat Science Association: Savoy, IL, 2001; pp 143–147.

(8) Josäll, Å.; Martinsson, L.; Tornberg, E. Possible mechanism for the effect of the *RN*<sup>-</sup> allele on pork tenderness. *Meat Sci.* **2003**, *64*, 341–350.

(9) Josäll, Å.; von Seth, G.; Tornberg, E. Sensory and meat quality traits of pork in relation to post-slaughter treatment and *RN* genotype. *Meat Sci.* **2003**, *66*, 113–124.

(10) Lindahl, G.; Enfält, A.-C.; von Seth, G.; Josell, Å.; Hedebro-Velander, I.; Andersen, H. J.; Braunschweig, M.; Andersson, L.; Lundström, K. A second mutant allele (VI991) at the *PRKAG3* (*RN*) locus – I. Effect on technological meat quality of pork loin. *Meat Sci.* **2004**, *66*, 609–619.

(11) Lindahl, G.; Enfält, A. C.; Andersen, H. J.; Lundström, K. Impact of *RN* genotype and storage time on colour characteristics of the pork muscles *longissimus dorsi* and *semimembranosus*. *Meat Sci.* **2006**, *74*, 746–755.

(12) Essén-Gustavsson, B.; Jensen-Waern, M. Metabolic profile in different tissues and postmortem glycogenolysis in skeletal muscle of pigs with different *PRKAG3* genotypes. In *Proceedings 53rd International Congress of Meat Science and Technology*, Beijing, China; China Agricultural University Press: Beijing, China, 2007; pp 221–222.

(13) Milan, D.; Jeon, J.-T.; Looft, C.; Amarger, V.; Robic, A.; Thelander, M.; Rogel-Gaillard, C.; Paul, S.; Iannuccelli, N.; Rask, L.; Ronne, H.; Lundström, K.; Reinsch, R.; Gellin, J.; Kalm, E.; Le Roy, P.; Chardon, P.; Andersson, L. A mutation in *PRKAG3* associated with excess glycogen content in pig skeletal muscle. *Science* **2000**, *288*, 1248–1251.

(14) Talmant, A.; Fernandez, X.; Sellier, P.; Monin, G. Glycolytic potential in longissimus dorsi muscle of Large White pigs as measured after in vivo sampling. In *Proceedings of the 35th International Congress of Meat Science and Technology*, Copenhagen, Denmark; Danish Meat Research Institute: Roskilde, Denmark, 1989; pp 1129–1132.

(15) Keppler, D.; Decker, K. Glycogen. Bestimmung mit Amyloglucosidase. In *Methoden der Enzymatische Analysen*, 2nd ed., Band II; Bergmeyer, H. U., Ed.; Verlag Chemie: Weinheim, Germany, 1970; pp 1127–1131.

(16) Bendall, J. R. Cold-contraction and atp-turnover in the red and white musculature of the pig, *post mortem*. *J. Sci. Food Agric.* **1975**, *26*, 55–71.

(17) Bax, A. A Spatially selective composite 90° radiofrequency pulse. *J. Magn. Reson.* **1985**, *65*, 142–145.

(18) Ancian, B.; Bourgeois, I.; Dauphin, J.-F.; Shaw, A. A. Artifact-free pure absorption PFG-enhanced DQF-COSY spectra including a gradient pulse in the evolution period. *J. Magn. Reson.* **1997**, *125*, 348–354.

(19) Tomasi, G.; van den Berg, F.; Andersson, C. Correlation optimized warping and dynamic time warping as pre-processing methods for chromatographic data. *J. Chemom.* **2004**, *18*, 231–241.

(20) Arús, C.; Bárány, M. Application of high-field <sup>1</sup>H-NMR spectroscopy for the study of perfused amphibian and excised mammalian muscles. *Biochim. Biophys. Acta* **1986**, *886*, 411–424.

(21) Roslund, M. U.; Tähtinen, P.; Niemitz, M.; Sjöholm, R. Complete assignment of the <sup>1</sup>H and <sup>13</sup>C chemical shifts and J<sub>H,H</sub> coupling constants in NMR spectra of D-glucopyranose and all D-glucopyranosyl-D-glycopyranosides. *Carbohydr. Res.* **2008**, *343*, 101–112.

(22) Hansen, P. I.; Larsen, F. H.; Motawia, S. M.; Blennow, A.; Spraul, M.; Dvortsak, P.; Engelsen, S. B. Structure and hydration of the amylopectin trisaccharide building blocks – synthesis, NMR and molecular dynamics. *Biopolymers* **2008**, *89*, 1179–1193.

(23) Larsen, F. H.; Blennow, A.; Engelsen, S. B. Starch granule hydration – a MAS NMR investigation. *Food Biophys.* **2008**, *3*, 25–32.

(24) Lemieux, R. U.; Stevens, J. D. The proton magnetic resonance spectra and tautomeric equilibria of aldoses in deuterium oxide. *Can. J. Chem.* **1966**, *44*, 249–262.

(25) Riek, R.; Fiaux, J.; Bertelsen, E. B.; Horwich, A. L.; Wüthrich, K. Solution NMR techniques for large molecular and supramolecular structures. *J. Am. Chem. Soc.* **2002**, *124*, 12144–12153.

(26) Mohanty, T. R.; Park, K. M.; Pramod, A. B.; Kim, J. H.; Choe, H. S.; Hwang, I. H. Molecular and biological factors affecting skeletal muscle cells after slaughtering and their impact on meat quality: a mini-review. *J. Muscle Foods* **2010**, *21*, 51–78.

(27) Roach, P. J. Glycogen and its metabolism. *Curr. Mol. Med.* **2002**, *2*, 101–120.

(28) Kylä-Puhju, M.; Ruusunen, M.; Puolanne, E. Activity of porcine muscle glycogen debranching enzyme in relation to pH and temperature. *Meat Sci.* **2005**, *69*, 143–149.

(29) Copenhafer, T. L.; Richert, B. T.; Schinkel, A. P.; Grant, A. L.; Gerrard, D. E. Augmented postmortem glycolysis does not occur early postmortem in AMPK $\gamma$ 3-mutated porcine muscle of halothane positive pigs. *Meat Sci.* **2006**, *73*, 590–599.